

NMR Relaxation Study of Ion Dynamics in Nanocrystalline and Polycrystalline LiNbO₃

D. Bork and P. Heitjans*

Institut für Physikalische Chemie und Elektrochemie und SFB 173, Universität Hannover, Callinstrasse 3-3a, 30167 Hannover, Germany

Received: March 17, 1998; In Final Form: July 23, 1998

Nanocrystalline (*n*) LiNbO₃ was prepared by high-energy ball milling from the polycrystalline (*p*) material. Grain sizes were determined by XRD measurements and TEM images; thermal stability ranges of the samples were examined by DTA. NMR investigations of the diffusion-induced ⁷Li spin-lattice relaxation (SLR) rate T_1^{-1} of n-LiNbO₃ in the temperature range from $T = 140$ to 460 K at frequencies between $\nu = 24$ and 78 MHz revealed a reduced activation energy on the low-temperature side of the typical peak in a $\log T_1^{-1}$ vs T^{-1} plot in comparison with results obtained from experiments performed on the p-material between 300 and 1400 K. Corresponding measurements of the SLR rate in the rotating reference frame yielded an asymmetric peak in the case of p-LiNbO₃, in contradiction to standard BPP theory, whereas in n-LiNbO₃ only a weakly temperature-dependent relaxation rate background was observed. Furthermore, neither in n- nor in p-LiNbO₃ BPP-type frequency dependencies of the SLR rate, i.e., $T_1^{-1} \propto \nu^{-\beta}$ with $\beta = 2$, were found. The determined values ranging from $\beta = 1.1$ to 1.5 are ascribed to the influence of structural disorder and Coulomb interaction on the diffusive motion.

Introduction

In contrast to amorphous systems displaying homogeneous structural disorder, nanocrystalline materials¹ are considered systems where structural disorder is heterogeneously distributed. Typical grain sizes in these materials range from 5 to 50 nm, resulting in two phases: one consisting of nanometer-sized crystallites separated by a large volume fraction of grain boundaries or interfacial regions which may contain up to 50% of the atoms.² The grains are regarded as small single crystals with perfect crystal structure, whereas the interfacial regions are showing a disordered structure. The dispersed crystalline phase is stabilizing the defect structure of the interfacial regions where the excess energy of this metastable system is stored. The nonequilibrium structure of the interfacial regions is responsible for special physical properties of these materials.

Despite extensive work in recent years involving many experimental techniques, nuclear magnetic resonance (NMR) has only been used in few cases to study the unique properties of nanocrystalline materials.^{1,2} Our main objective was to investigate the effect of the heterogeneous structure—introduced by mechanical attrition—of a nanocrystalline ceramic material on NMR signals, i.e., to find out whether NMR, via temperature-dependent measurements, is able to (i) distinguish between the two different structural regions and (ii) can differentiate between ion diffusion in these distinct areas. Here, we focus on ⁷Li spin-lattice relaxation (SLR) rate measurements and, thus, on the dynamical aspects of our model system LiNbO₃. Some results from NMR spectra, i.e., ⁷Li line shape studies, emphasizing the structural properties of these samples as well as the first discussion of the diffusion-induced narrowing of the central line in the ⁷Li spectra have been presented in a previous note.³

Measuring the temperature dependence of the SLR rate provides information about dynamical properties such as the activation energy and the jump rate of ionic motion (see, e.g., ref 4 for a brief introduction). Whereas the activation energy of short-range motion can be extracted from the slope of the

low-temperature side of the peak in the Arrhenius-type $\log T_1^{-1}$ vs T^{-1} plot, the high-temperature side reveals the activation energy of long-range diffusion. The fact that different regimes indicating different kinds of motion can be distinguished in a $\log T_1^{-1}$ vs T^{-1} plot is a consequence of the temperature dependence of the correlation time τ_c , which is the time constant characterizing the nuclear magnetic field fluctuations caused by diffusing ions. τ_c is a direct measure of the mean atomic residence time and normally related to temperature via an Arrhenius relation. τ_c can be determined via the condition $\omega\tau_c = 0.62^5$ for the maximum of the $T_1^{-1}(T)$ curve measured at the NMR frequency $\nu = \omega/2\pi$. The diffusion coefficient is obtained from τ_c via the Einstein-Smoluchowski equation. Aiming to observe the maximum and the high-temperature side in LiNbO₃, SLR experiments in the rotating reference frame in addition to SLR measurements in the laboratory reference frame were performed because in the latter case the maximum could not be reached below 1400 K for the p-sample and below 460 K for the n-sample.

Samples and Measurement Conditions

Besides the “classic” method of preparing nanocrystalline materials by noble gas condensation,¹ high-energy ball milling⁶—among others—has become an alternative technique in which small grain sizes are achieved by mechanical attrition of a coarser grained source material. We used a SPEX 8000 ball mill to prepare several nanocrystalline samples in an Al₂O₃ vial set. By varying the milling time between 0.5 and 128 h, average grain sizes between 105 and 16 nm were obtained. Here, we focus on a sample which was milled for 16 h, resulting in an average grain size of 23 nm, as determined by XRD measurements. This is in agreement with the results obtained from TEM images for the same sample. DTA showed a characteristic broad exothermic peak indicating grain boundary relaxation and grain growth above 510 K. Since (i) DTA is a dynamical technique and (ii) grain boundary relaxation and grain growth cannot be

ascribed to definite transition temperatures, this value has to be regarded as an upper limit concerning the accessible temperature range for NMR experiments. To prevent grain boundary relaxation and grain growth during NMR data acquisition, i.e., to ensure reproducibility of the results, tests were performed which proved that NMR measurements on nanocrystalline LiNbO₃ samples had to be restricted to temperatures below 460 K. Compaction of the sample at room temperature using a pressure of 1.25 GPa revealed no effect on the NMR results when compared with measurements on an as-prepared, i.e., not compacted, sample.

For preparing nanocrystalline samples, we used polycrystalline LiNbO₃ with a purity of 99.99% commercially available from Aldrich. It consists of crystallites with grain sizes between 0.6 and 6 μm , as determined from TEM images. Neither DTA investigations between 300 and 960 K nor NMR studies up to 1400 K gave any hints for thermally induced changes such as phase transitions in the sample. According to a chemical analysis delivered by Aldrich, the material contains 54.9 mol % niobium, indicating nonstoichiometry.⁷ Comprehensive NMR measurements on this material served for reference purposes because no relevant SLR rate data of LiNbO₃ have been reported in the literature yet.

Measurements of the SLR time T_1 of ⁷Li in the laboratory reference frame at 24 and 39 MHz were performed using a Bruker MSL 100 console with an internal 200 W power amplifier and a tunable Oxford 7 T cryomagnet with a 89 mm bore. T_1 experiments at 78 MHz as well as measurements of the SLR time T_{1e} in the pulsed rotating reference frame were done using a Bruker MSL 200 spectrometer with an internal 200 W amplifier and a cryomagnet at fixed field. In the temperature range from 140 to 460 K, commercial Bruker probe heads were used, while higher temperatures up to 1400 K were adjusted through home-built probe heads.

In p-LiNbO₃ samples, one deals with SLR times T_1 up to a few hundred seconds. From a practical point of view, this fact makes the use of time-saving pulse sequences a must. For that reason, we chose the saturation recovery pulse sequence ($n \cdot \pi/2 - \tau - \pi/2$) for measuring the SLR time T_1 in the laboratory reference frame. For measurements in the kilohertz regime, we performed T_{1e} experiments in a pulsed rotating reference frame, which are reported to be a time-saving alternative for conventional $T_{1\rho}$ experiments in the rotating frame.⁸

The time evolution of the nuclear magnetization was fitted by a single exponential in all T_1 experiments as well as in the T_{1e} measurements on p-LiNbO₃, whereas in the case of T_{1e} measurements on n-LiNbO₃, the transients could be described by stretched exponentials

$$M(t) = M(0) \exp\left[-\left(\frac{t}{T_{1e}}\right)^\alpha\right] \quad (1)$$

with $\alpha = 0.3$. The fit function (eq 1) exhibits the possibility of quantifying the experimental data rather than revealing characteristic physical properties of the n-material. An alternative approach would be fitting the transients by a sum of two exponentials according to the heterogeneous structure of the n-system. This would involve the additional, but experimentally not proven, assumption of the independence of the two spin reservoirs, i.e., the grains and the grain boundaries.

Results and Discussion

p-LiNbO₃. In Figure 1 results from ⁷Li SLR measurements performed in the laboratory reference frame on the p-LiNbO₃

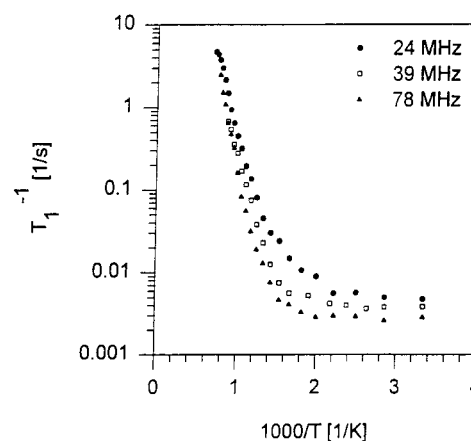


Figure 1. ⁷Li SLR rate versus inverse temperature in p-LiNbO₃ at three frequencies measured in the laboratory reference frame.

sample at three frequencies are presented. Below 500 K, a frequency-dependent but temperature-independent relaxation rate background is observed. Above 500 K, a pronounced diffusion-induced low-temperature side arises. From its slope, a frequency-independent activation energy of 0.75 eV is determined. The observed frequency dependence of the SLR rate according to

$$T_1^{-1} \propto \nu^{-\beta} \quad (2)$$

with $\beta \approx 1.2$ is the first indication of a deviation from standard BPP behavior⁹ which requires $\beta = 2$.

Since the SLR rate maximum could not be reached in the experimentally accessible temperature range up to 1400 K, additional measurements in the rotating reference frame at seven frequencies in the kilohertz regime were performed in order to "shift the plot to lower temperatures". The corresponding data for four selected frequencies are plotted in Figure 2A with the 24 MHz curve from Figure 1 for comparison. Besides the maxima of the curves, parts of their high-temperature sides are also detectable. To reveal more details, an enlarged section of the peaks is shown in Figure 2B. The activation energy of 0.75 eV calculated from their low-temperature sides, which applies to short-range motion, fully agrees with the result from Figure 1. On the high-temperature side, an activation energy of 0.88 eV due to long-range diffusion indicates a deviation from a symmetric peak shape and is, thus, incompatible with standard BPP theory. The frequency dependence with $\beta \approx 1.5$ on the low-temperature side is in agreement with the results from the laboratory reference frame.

As stated above, it is possible to determine a diffusion coefficient from the maximum condition by using the Einstein-Smoluchowski equation

$$D = \frac{\langle x^2 \rangle}{2d\tau_c} \quad (3)$$

where $\langle x^2 \rangle$ is the mean-square displacement as calculated from an Li-Li distance of approximately 0.38 nm¹⁰ in the crystal structure of LiNbO₃ and d is the dimensionality of the jump process; here, d is supposed to be 3 because a frequency-dependent SLR rate on the high-temperature side indicating low dimensionality of Li-ion motion (see, e.g., ref 11) is absent. For $T = 890$ K, $\omega = 1.9 \times 10^5 \text{ s}^{-1}$, i.e., $\tau_c = 3.2 \times 10^{-6} \text{ s}$, one obtains a diffusion coefficient of $D = 7.5 \times 10^{-15} \text{ m}^2/\text{s}$.

n-LiNbO₃ and Comparison with p-LiNbO₃. Figure 3 displays the results from SLR rate measurements on n-LiNbO₃ in the laboratory reference frame. In comparison with the

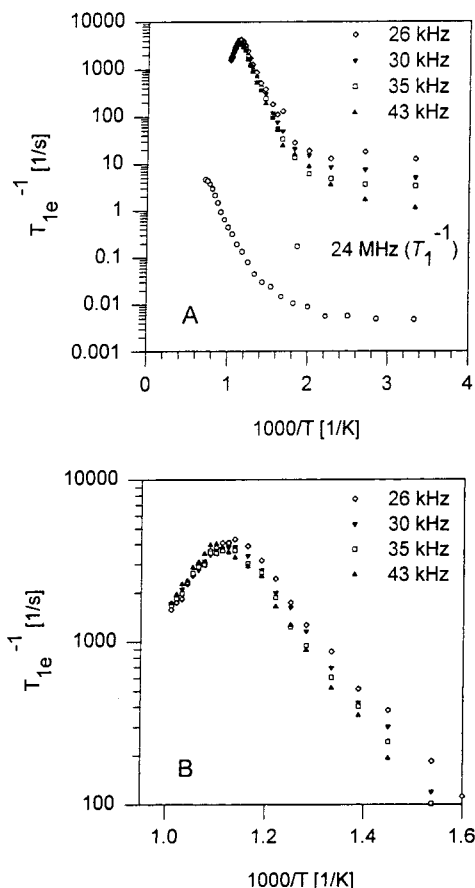


Figure 2. (A) ^7Li SLR rate versus inverse temperature in p-LiNbO₃ at four frequencies measured in the pulsed rotating reference frame. For comparison the T_1^{-1} results at 24 MHz are also displayed. (B) Enlarged presentation of the peak of the ^7Li SLR rate in p-LiNbO₃.

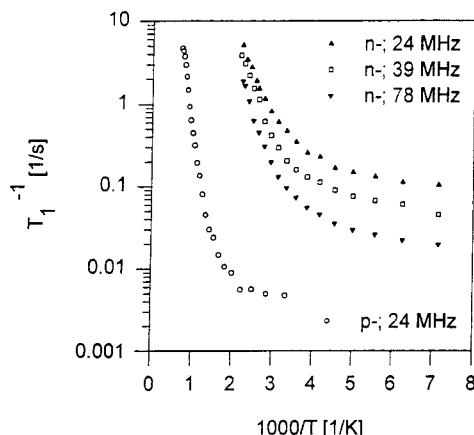


Figure 3. ^7Li SLR rate versus inverse temperature in n-LiNbO₃ at three frequencies measured in the laboratory reference frame. For comparison the T_1^{-1} results from p-LiNbO₃ at 24 MHz are displayed, too.

p-material, the diffusion-induced low-temperature side is shifted to lower temperatures and reflects a reduced activation energy of 0.27 eV, both indicating a higher ion mobility in the n-system. This value for the activation energy has to be regarded as a lower limit because it is not sure whether the steepest part of the low-temperature side is already reached at 460 K. Furthermore, in contrast to p-LiNbO₃, the data indicate a temperature dependence of the background SLR rate. The value of $\beta = 1.1$ found for the frequency dependence of the SLR rate on the low-temperature side reveals a deviation from BPP theory, too.

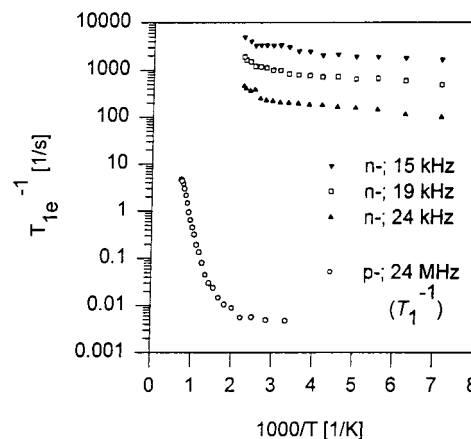


Figure 4. ^7Li SLR rate versus inverse temperature in n-LiNbO₃ at three frequencies measured in the pulsed rotating reference frame. For comparison the T_1^{-1} results from p-LiNbO₃ at 24 MHz are also displayed.

Figure 4 displays the results from the T_{1e} experiments on n-LiNbO₃ in the rotating reference frame. Again, a small temperature dependence of the background SLR rate is indicated. The determination of an activation energy is not possible because only the onset of the diffusion-induced low-temperature side can be detected.

Referring to our objective to investigate the influence of heterogeneous structural disorder on ion dynamics, we obtained the following results. The reduction of the effective activation energy observed in n-LiNbO₃ to about one-third of the value obtained for the reference system p-LiNbO₃ and, thus, the enhancement of Li diffusivity is ascribed to the higher ion mobility in the interfacial regions. Besides a higher relaxation rate background, a pronounced shift of the low-temperature side is detected, indicating the onset of diffusion at considerably lower temperatures. As a result of introducing a high density of interfacial regions due to mechanical attrition, an additional diffusion mechanism is observed in the n-material. The presumption that a second mechanism instead of just a modification of the original diffusion process is observed is based on ^7Li NMR line shape studies performed on the same samples, which allow us to clearly identify two different contributions to the overall ion mobility.³

The detected frequency dependencies of the diffusion-induced relaxation rate being characterized by values of β in the range from 1.1 to 1.5 can, e.g., be interpreted by the jump relaxation model¹² in both the p- and the n-material. The results for p-LiNbO₃ can be ascribed to homogeneous disorder due to the inherent nonstoichiometry and the resulting high concentration of vacancies in the lithium sublattice. This kind of (assumed) homogeneous disorder due to nonstoichiometry in a crystal lattice has to be distinguished from the homogeneous structural disorder of glassy systems, which is a property independent of stoichiometry. Because of this inherent nonstoichiometry also existing in n-LiNbO₃, the influence of the heterogeneous structural disorder on the frequency dependence of the SLR rate cannot be distinguished from the above-mentioned homogeneous disorder due to the defect structure in the lithium sublattice. Furthermore, in conjunction with disorder, Coulomb interaction between the moving ions has been shown to be essential in explaining non-BPP-type SLR behavior.¹³

The small temperature dependence of the SLR rate background observed in n-LiNbO₃ is similar to that obtained from measurements on glassy ionic conductors,¹⁴ probably revealing common features of homogeneous and heterogeneous structural

disorder. Further research work concerning the SLR rate at low temperatures is required.

In conclusion, the present investigation demonstrated that temperature-dependent NMR measurements can provide valuable information concerning the characterization of structural and dynamical properties of nanocrystalline materials.

Acknowledgment. We thank Dr. G. Balzer for useful discussions. This work was supported by the Deutsche Forschungsgemeinschaft (DFG) and the Fonds der Chemischen Industrie.

References and Notes

- (1) Gleiter, H. *Prog. Mater. Sci.* **1989**, 33, 223.
- (2) Siegel, R. W. *Encyclopedia of Applied Physics* **1994**, 11, 173.
- (3) Bork, D.; Heitjans, P. In *28th Congress Ampere on Magnetic Resonance and Related Phenomena*; Smith, M. E., Strange, J. H., Eds.; ISBN 0904938913, University of Kent: Canterbury, 1996; p 418.
- (4) Schatz, G.; Weidinger, A. *Nuclear Condensed Matter Physics: Nuclear Methods and Applications*; Wiley: Chichester, 1996.
- (5) Slichter, C. P. *Principles of Magnetic Resonance*; Springer: Berlin, 1990.
- (6) Fecht, H.-J. *Nanophase Materials*; Hadjipanayis, G. C., Siegel, R. W., Eds.; Kluwer Academic Publishers: Netherlands, 1994; p 125.
- (7) Svaasand, L. O.; Eriksrud, M.; Grand, A. P.; Mo, F. *J. Cryst. Growth* **1973**, 18, 179.
- (8) Rhim, W.-K.; Burum, D. P.; Ellemann, D. D. *J. Chem. Phys.* **1978**, 68, 692.
- (9) Bloembergen, N.; Purcell, E. M.; Pound, R. V. *Phys. Rev.* **1948**, 73, 679.
- (10) *Gmelins Handbuch der Anorganischen Chemie*, Niob, Teil B4; Verlag Chemie: Weinheim, 1973.
- (11) Küchler, W.; Heitjans, P. *Solid State Ionics* **1994**, 70/71, 434.
- (12) Funke, K. *Prog. Solid State Chem.* **1993**, 22, 111.
- (13) Meyer, M.; Maass, P.; Bunde, A. *Phys. Rev. Lett.* **1993**, 71, 573.
- (14) Franke, W.; Heitjans, P. *Ber. Bunsen-Ges. Phys. Chem.* **1992**, 96, 1674.